

# Eigenstate Thermalization, Random Matrix Theory, and Behemoths

Ivan M. Khaymovich,<sup>1</sup> Masudul Haque,<sup>1,2</sup> and Paul A. McClarty<sup>1</sup>

<sup>1</sup>Max Planck Institute for the Physics of Complex Systems, Nöthnitzer Straße 38, 01187 Dresden, Germany

<sup>2</sup>Department of Theoretical Physics, Maynooth University, W23 F2H6 Co. Kildare, Ireland

 (Received 10 July 2018; revised manuscript received 13 November 2018; published 19 February 2019)

The eigenstate thermalization hypothesis (ETH) is one of the cornerstones of contemporary quantum statistical mechanics. The extent to which ETH holds for nonlocal operators is an open question that we partially address in this Letter. We report on the construction of highly nonlocal operators, behemoths, that are building blocks for various kinds of local and nonlocal operators. The behemoths have a singular distribution and width  $w \sim \mathcal{D}^{-1}$  ( $\mathcal{D}$  being the Hilbert space dimension). From there, one may construct local operators with the ordinary Gaussian distribution and  $w \sim \mathcal{D}^{-1/2}$  in agreement with ETH. Extrapolation to even larger widths predicts sub-ETH behavior of typical nonlocal operators with  $w \sim \mathcal{D}^{-\delta}$ ,  $0 < \delta < 1/2$ . This operator construction is based on a deep analogy with random matrix theory and shows striking agreement with numerical simulations of nonintegrable many-body systems.

DOI: [10.1103/PhysRevLett.122.070601](https://doi.org/10.1103/PhysRevLett.122.070601)

*Introduction.*—Some of the most fundamental questions in quantum statistical mechanics relate to whether and how thermalization occurs in isolated quantum systems out of equilibrium. Whereas a closed quantum system in a pure state never comes to thermal equilibrium, subsystems may thermalize in the sense that observables acting on the subsystem may be computed from a thermal ensemble in the long time limit. The process of thermalization depends on the nature of the many-body system, the initial state, the subsystem, and the observable. Despite the complexity of this problem, the eigenstate thermalization hypothesis (ETH) boils the issue down to the nature of the matrix element distribution of the observable in the eigenstate basis. ETH is the conjecture that the fluctuations of these matrix elements are exponentially small in the system size [1–15]. Denoting eigenvalues and eigenstates by  $\mathbf{E}_A$  and  $|\mathbf{E}_A\rangle$ , ETH for an operator  $\hat{O}$  is stated as

$$\langle \mathbf{E}_A | \hat{O} | \mathbf{E}_B \rangle = \delta_{AB} f_O^{(1)}(\bar{\mathbf{E}}) + e^{-S(\bar{\mathbf{E}})/2} f_O^{(2)}(\bar{\mathbf{E}}, \omega) R_{AB}, \quad (1)$$

where  $S \sim \log \mathcal{D}$  is the entropy and  $\mathcal{D}$  is the Hilbert space dimension,  $\bar{\mathbf{E}} = (1/2)(\mathbf{E}_A + \mathbf{E}_B)$  and  $\omega = \mathbf{E}_B - \mathbf{E}_A$ ,  $R_{AB}$  is a random variable with zero mean and unit variance, and  $f^{(1,2)}$  are smooth functions. A crucial aspect of ETH is the scaling of the width of the operator distribution: the width of the distribution falls off as  $e^{-S(\bar{\mathbf{E}})/2} \sim \mathcal{D}^{-1/2}$ . This scaling is based on the similarity between typical many-body eigenstates and random states [16–18].

Evidence from a large number of numerical studies strongly suggests that ETH is satisfied for typical states of generic nonintegrable systems and for physical observables [13–38]. However, there is currently little sharp understanding of the class of operators which satisfy

ETH. While local observables are expected to obey ETH, one might imagine that sufficiently nonlocal operators are athermal because there is no distinction between the subsystem and the bath. Projection operators onto eigenstates are extreme examples of this type. Earlier work related to nonlocal operators in the ETH context includes Refs. [34,39–42].

In this Letter, we explore a correspondence between Gaussian random matrices (GRM) governed by random matrix theory (RMT) and many-particle quantum systems that allows one to make testable predictions for the scaling of matrix element distributions of fairly general operators. Figure 1 summarizes our classification of operators. We begin by considering a class of highly nonlocal operators that connect single pairs of many-body configurations. We

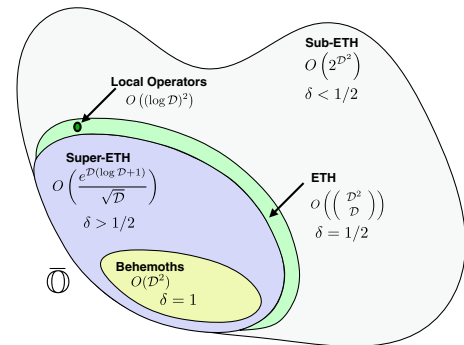


FIG. 1. Schematic showing the space of operators  $\bar{\mathcal{O}}$  having elements zero or unity in the configuration basis. The operators within  $\bar{\mathcal{O}}$  are organized into classes distinguished by the scaling of the width  $\sigma \sim \mathcal{D}^{-\delta}$  of matrix element distributions in the eigenstate basis. The number of each class of operators is shown using the big- $\mathcal{O}$  notation.

will call these behemoth operators. Using RMT, we analytically derive the distribution of eigenstate matrix elements of behemoths. We demonstrate that behemoths in a wide class of lattice many-body systems match the RMT predictions. We show that these operators are distinguished by exhibiting *super*-ETH scaling with eigenstate distribution width scaling as  $\mathcal{D}^{-1}$ .

The behemoth operators have a deeper importance: they are building blocks for a vastly larger class of operators that includes the local operators. By connecting more and more pairs of many-body configurations, one can tune the scaling of the matrix element distribution to be  $\mathcal{D}^{-\delta}$ . The *super*-ETH operators have  $1/2 < \delta \leq 1$ , the operators that obey ETH (such as local operators) have  $\delta = 1/2$  and the *sub*-ETH operators have  $\delta < 1/2$ . As with behemoth operators, RMT supplies predictions for the distribution of all such operators that we compare with numerical results for many-body Hamiltonians. This construction is an alternative route to the  $\mathcal{D}^{-1/2}$  (ETH) scaling of local operators.

Figure 1 summarizes our results using a schematic of the space of operators (restricted to those with elements zero and one in the operator matrix),  $\bar{\mathcal{O}}$ . The sizes of different subsets of operators within  $\bar{\mathcal{O}}$  are indicated, together with the scalings that we have derived using random matrix calculations and tested numerically on many-body systems.

*Analogy between random matrix theory and many-body physics.*—Suppose  $H_{ij}$  is a  $N \times N$  GRM with eigenstates  $|E_\alpha\rangle$ . This can be interpreted as a single particle hopping Hamiltonian on a fully connected network, with “node” indices  $i, j$ . We also consider a  $\mathcal{D} \times \mathcal{D}$  many-body lattice Hamiltonian  $H_{\mathbf{n}\mathbf{n}'}$  with eigenstates  $|E_A\rangle$ . Each  $\mathbf{n}$  is a many-body configuration, specified by the occupancies of the  $L$  lattice sites. RMT predictions apply directly for the single-particle system, since  $H_{ij}$  is a GRM. To apply these predictions to the many-particle system, we need to replace nodes  $i, j$  by configurations  $\mathbf{n}, \mathbf{n}'$  and  $N$  by  $\mathcal{D}$ . Unlike  $H_{ij}$ , the many-body Hamiltonian matrix  $H_{\mathbf{n}\mathbf{n}'}$  is sparse and its elements are not truly random. Nevertheless, nonintegrable many-body Hamiltonians generally follow many RMT predictions, e.g., (a) the energy eigenvalues  $\{E_\alpha\}$  display Wigner-Dyson level statistics, like their GRM counterparts  $\{E_A\}$ , and (b) the eigenstate coefficients  $U_{A,\mathbf{n}} \equiv \langle \mathbf{n} | E_A \rangle$  form dense matrices with approximately Gaussian-distributed elements [43], like their GRM counterparts  $u_{\alpha,i} \equiv \langle i | E_\alpha \rangle$ .

For the single-particle system, the natural operators to consider are  $\hat{w}_{ij} \equiv \hat{a}_i^\dagger \hat{a}_j$ , node-to-node hopping operators. The corresponding operators in the many-body model each connect one pair of many-body configurations:

$$\hat{\Omega}_{\mathbf{n}\mathbf{n}'} \equiv |\mathbf{n}\rangle\langle \mathbf{n}'|. \quad (2)$$

As these are extremely nonlocal, we call them behemoth operators. The matrix representation of  $\hat{\Omega}_{\mathbf{n}\mathbf{n}'}$  in the

configuration basis has only one nonzero entry:  $\langle \mathbf{m} | \hat{\Omega}_{\mathbf{n}\mathbf{n}'} | \mathbf{m}' \rangle = \delta_{\mathbf{m}\mathbf{n}} \delta_{\mathbf{m}'\mathbf{n}'}$ . Behemoths thus form a basis for all operators. Hermitian counterparts of behemoths,  $\hat{\Gamma}_{\mathbf{n}\mathbf{n}'} \equiv \hat{\Omega}_{\mathbf{n}\mathbf{n}'} + \hat{\Omega}_{\mathbf{n}'\mathbf{n}}$ , have two nonzero entries.

We will examine the distribution of eigenstate matrix elements of behemoths. We propose that the statistics of such many-body matrix elements match those of the matrix elements of  $\hat{w}_{ij} = \hat{a}_i^\dagger \hat{a}_j$  in GRM. Below, we calculate their distribution on the GRM side and then carry out numerical tests of the correspondence.

If the many-body Hamiltonian conserves particle number  $N_p$ , then for spinless fermions or hard-core bosons the many-body matrix elements of the behemoths are

$$\Omega_{\mathbf{n}\mathbf{n}'}^{AB} \equiv \langle E_A | \hat{\Omega}_{\mathbf{n}\mathbf{n}'} | E_B \rangle = \langle E_A | \prod_{k=1}^{N_p} \hat{c}_{r_k}^\dagger \hat{c}_{s_k} | E_B \rangle. \quad (3)$$

The Behemoth changes one configuration of  $N_p$  particles into another. Here  $\{r_k\}$  ( $\{s_k\}$ ) is the set of distinct sites occupied in configuration  $\mathbf{n}$  ( $\mathbf{n}'$ ). (Some sites might be occupied in both  $\mathbf{n}$  and  $\mathbf{n}'$  configurations [44].) For spin-1/2 systems, spins up (down) are interpreted as occupied (empty) sites and  $N_p$  is the number of up spins. Equation (3) can be readily generalized to cases where multiple occupancies are allowed (e.g., bosonic or fermionic Hubbard models, or  $S > 1/2$  spin systems), and to systems where particle number is not conserved [44].

*From nonlocal to local.*—Besides  $\hat{\Omega}_{\mathbf{n}\mathbf{n}'}$ , we consider operators with varying degrees of locality,  $\hat{\Omega}_M = \prod_{k=1}^n \hat{c}_{r_k}^\dagger \hat{c}_{s_k}$ , which hop  $n$  of the  $N_p$  particles ( $n \lesssim N_p$ ). The expectation values of  $\hat{\Omega}_M$  are  $(2n)$ -point correlators. (For simplicity we consider the sets  $\{r_k\}$  and  $\{s_k\}$  to have no intersection.) Whereas  $\hat{\Omega}_{\mathbf{n}\mathbf{n}'}$  couples exactly two configurations,  $\hat{\Omega}_M$  changes the configuration on  $2n$  sites while the remaining sites may adopt any of

$$M \equiv \binom{L - 2n}{N_p - n}$$

configurations. The matrix representing  $\hat{\Omega}_M$  thus has  $M$  nonzero elements, each equal to 1; i.e.,  $\hat{\Omega}_M = \sum_{j=1}^M \hat{\Omega}_{\mathbf{n}_j, \mathbf{n}'_j}$  is a sum of  $M$  behemoths [46]. The behemoths themselves correspond to  $n = N_p$ , with  $M = 1$ . The limit of a local single particle hopping operator is  $n = 1$ . Local operators are thus formed by combining  $M = O(\mathcal{D})$  behemoths.

*Statistics of many-body operators from RMT.*—We now make concrete predictions using RMT. The GRM objects corresponding to the matrix elements of Eq. (3) are  $\omega_{ij}^{\alpha\beta} = \langle E_\alpha | \hat{a}_i^\dagger \hat{a}_j | E_\beta \rangle = u_{\alpha,i}^* u_{\beta,j}$ .

We first focus on Gaussian orthogonal ensemble (GOE) matrices. For sufficiently large matrix sizes  $N$ , coefficients of eigenstates  $u_{n,i}$  are real-valued independent Gaussian

variables with zero mean and variance  $\sigma_1^2 = 1/N$  [47–50]. The distribution is  $P_u(u) = e^{-u^2/2\sigma_1^2}/\sqrt{2\pi\sigma_1^2}$ . Within this approximation, both the diagonal ( $\alpha = \beta$ ) and off-diagonal ( $\alpha \neq \beta$ ) matrix elements of  $\hat{\omega}_{ij}$  have the distribution

$$P_\omega(x) = \int_{-\infty}^{\infty} du_1 du_2 P_u(u_1) P_u(u_2) \delta(x - u_1 u_2) = \frac{1}{\pi\sigma_1^2} K_0\left(\frac{|x|}{\sigma_1^2}\right). \quad (4)$$

Here  $K_\nu(x)$  is the modified Bessel function of the second kind. For the Hermitian counterpart  $\gamma_{ij}^{\alpha\beta} = \omega_{ij}^{\alpha\beta} + \omega_{ji}^{\alpha\beta}$  we distinguish between diagonal matrix elements ( $\alpha = \beta$ ) for which we obtain  $P_{\gamma,\text{diag}}(y) = P_\omega(y/2)/2$  and off-diagonal matrix elements ( $\alpha \neq \beta$ ) for which we must convolve two distributions of the form (4) giving [45]

$$P_\gamma(y) = \frac{1}{2\pi} \int_{-\infty}^{\infty} e^{-iqy} \frac{dq}{1 + \sigma_1^4 q^2} = \frac{e^{-|y|/\sigma_1^2}}{2\sigma_1^2}. \quad (5)$$

Next we look at sums of  $M$  operators of type  $\hat{\omega}_{ij}$  and calculate the distribution of diagonal and off-diagonal matrix elements. The Fourier transform  $\tilde{P}_{\omega_M}(q)$  of  $P_{\omega_M}(X)$  is the  $M$ th power of  $\tilde{P}_\omega(q) = (1 + \sigma_1^4 q^2)^{-1/2}$  [45]. This leads to

$$P_{\omega_M}(X) = \frac{1}{\sqrt{\pi}\Gamma[M/2]\sigma_1^2} \left(\frac{|X|}{2\sigma_1^2}\right)^{[(M-1)/2]} K_{[(1-M)/2]} \left(\frac{|X|}{\sigma_1^2}\right). \quad (6)$$

This function is Gaussian for large enough  $M$ :  $P_{\omega_M}(X) \approx e^{-X^2/(2M\sigma_1^4)}/\sqrt{2\pi M\sigma_1^2}$ , in accordance with the central limit theorem. The variance of this distribution is  $M\sigma_1^2 \sim MN^{-2}$  which goes as  $1/N$  for  $M \sim N$ .

The distribution of the Hermitian analog,  $\hat{\gamma}_{M'}$  for off-diagonal matrix elements is Eq. (6) with  $M = 2M'$ . The distribution for diagonal elements of  $\hat{\gamma}_{M'}$  is  $P_{\omega_M}(Y/2)$  with  $M = M'$ .

The analysis for the GUE case is similar [45]. The off-diagonal matrix elements are now complex; the marginal distributions for real and imaginary parts of  $\omega_{ij}^{\alpha\beta}$  have exponential form. The amplitude has the distribution

$$P_{|\omega|}(x) = \frac{x}{\sigma_2^4} K_0\left(\frac{x}{\sigma_2^2}\right), \quad (7)$$

which vanishes for  $x \rightarrow 0$ . Here  $\sigma_2^2 = 1/(2N)$ . Other GUE and GSE distributions are derived for completeness in Ref. [45].

We now discuss these results in light of the correspondence with many-body physics. For eigenstates in the middle of the spectrum of a local nonintegrable model—those for which the energy dependence of the states is

weakest—we expect that the off-diagonal matrix elements of Behemoth operators of the type (3) should be distributed according to Eq. (4), or according to Eq. (7) if time reversal symmetry is violated. Similarly, Hermitian counterparts to behemoths, and diagonal matrix elements should follow the corresponding RMT distributions outlined above. The width  $\sigma_1^2 = 1/N$  in GRM becomes  $1/\mathcal{D}$  in the many-body case. The behemoths thus obey a *super-ETH* scaling behavior. Then, by tuning  $M$  in Eq. (6) we interpolate between Behemoth operators for  $M = 1$  to local one-particle hopping operators for

$$M = \begin{pmatrix} L - 2 \\ N_p - 1 \end{pmatrix}$$

where there is particle number conservation and  $M = 2^{L-2}$  otherwise. The width of local operator distributions scales as  $\sqrt{MD^{-2}} \sim \mathcal{D}^{-1/2}$ , as enshrined in the usual statement of ETH. Here, we have made predictions for the whole distributions of classes of local and nonlocal operators with no fitting parameters.

*Numerical results.*—We now present numerical tests of the conjectures described above. We performed these tests on an array of different interacting many-body lattice systems, including spin-1/2 chains, bosonic Hubbard models, and interacting spinless fermions. Data for three different systems appear in Figs. 2 and 4 while further comparisons (with specifications of the models) appear in Ref. [45]. Figure 2 shows the computed distributions (histograms) of off-diagonal matrix elements of Behemoth operators for a GOE case (spin chain) and a GUE case (Bose-Hubbard ladder with a magnetic field piercing every plaquette). Figures 2(a) and 2(b) use a single Behemoth and 20% of the midspectrum eigenstates of the system. Because particular operators may have atypical behavior, in Fig. 2(c) and the rest of the Letter we use statistics from a random set of between 50 and 500 behemoths, the matrix elements are typically calculated between the central 50–200 eigenstates. Owing to the greater abundance of data for off-diagonal matrix elements we present these here and show results for diagonal matrix elements—which have the same scaling—in Ref. [45].

The agreement in Fig. 2 with RMT predictions, Eqs. (4), (5), and (7), is excellent. The same is true for all systems we have tested, for both off-diagonal and diagonal matrix elements [45], as long as the systems are in nonintegrable (ergodic) regimes.

We next consider operators interpolating between behemoths and local operators, i.e.,  $(2n)$ -point correlators, with  $n = N_p$  for behemoths and  $n = 1$  for local operators. These correspond to increasing  $M$ , the number of nonzero elements in the operator matrix. Distributions of matrix elements are shown in Figs. 3(a)–3(c) for the spin chain, for  $n = N_p$ ,  $n = N_p - 1$ , and  $n = 1$ . The distribution goes from exponential to Gaussian as  $M$  increases. The scaling is

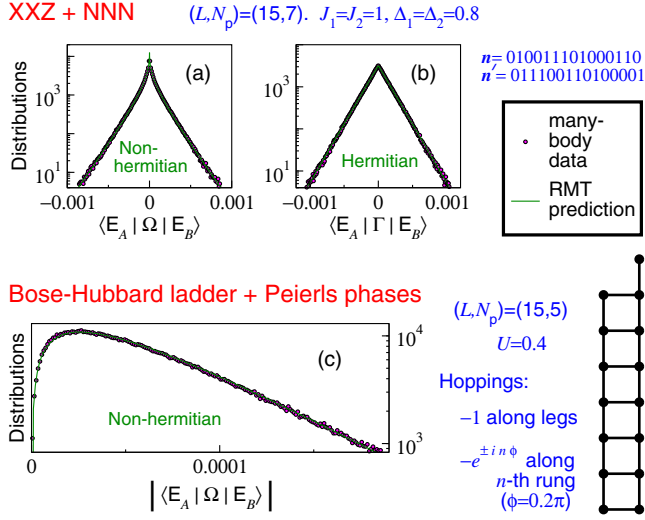


FIG. 2. Probability distributions of matrix elements of Behemoth operators, for two different many-body systems, compared with GOE and GUE predictions. (a),(b) Spin-1/2 chain with anisotropic Heisenberg (XXZ) couplings. Nearest-neighbor (NN) and next-nearest-neighbor (NNN) coupling strengths ( $J_{1,2}$ ) and anisotropies ( $\Delta_{1,2}$ ) are indicated. (c) Bose-Hubbard ladder (geometry in sketch) subject to magnetic field. Solid lines in (a),(b),(c) are predictions from Eqs. (4), (5), and (7), respectively.

$\sim \mathcal{D}^{-1}$  (super-ETH) for behemoths and  $\sim \mathcal{D}^{-1/2}$  for  $n = 1$ , Fig. 3(d).

At moderate  $M$  the agreement with Eq. (5) is excellent. A striking effect is seen at large  $M$ : the local operator distribution has the Gaussian shape and  $\mathcal{D}^{-1/2}$  scaling predicted by RMT, Eq. (5), but the width is systematically larger by a factor of order 1 [Figs. 3(c) and 3(d)]. This discrepancy is due to the presence of weak correlations in the eigenstates [45]. Correlation effects result in a remarkable *partial* violation of the central limit theorem.

Whereas  $M < O(\mathcal{D})$  operators have super-ETH scaling, we can also construct operators with sub-ETH scaling. By filling  $M \sim \mathcal{D}^{1+\beta}$  elements [ $\beta \in (0, 1)$ ] of the operator matrix, we obtain “dense” operators with matrix element distributions having widths  $\sim \sqrt{M\mathcal{D}^{-1}} \sim \mathcal{D}^{-1/2+\beta/2}$ . Two examples are shown in Fig. 3(e); the predictions are borne out by the numerical results.

*Exceptions to RMT scaling.*—We have shown that the correspondence between GRM and many-body operator distributions works very well for the vast majority of eigenstates and typical behemoths in nonintegrable models. Under exceptional circumstances, it can be made to fail. For example, if one or both of the configurations  $|\mathbf{n}\rangle$ ,  $|\mathbf{n}'\rangle$  in Eq. (2) are such that they predominantly have weight in the highest- or lowest-energy eigenstates, then the corresponding behemoth  $\Omega_{\mathbf{n}\mathbf{n}'}$  will have anomalously small matrix elements for midspectrum eigenstates. Maximally ferromagnetic configurations for a spin chain can lead to such anomalies [45].

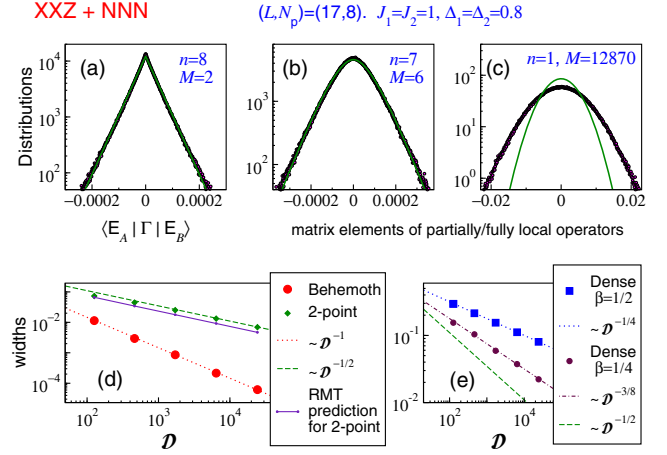


FIG. 3. (a),(b),(c) Distributions for Hermitian operators ( $2n$ -point correlators) of varying locality, from behemoth (a) to 2-point correlator (c). Number of nonzero terms  $M = 2M'$  in the operator matrix are shown. Solid lines are RMT predictions, Eq. (6). (d) Width of distributions for behemoths and local operators. The  $\sim \mathcal{D}^{-1}$  line is the RMT prediction for behemoths, Eq. (5). RMT prediction for local operators (solid line) falls below the data, consistent with panel (c). (e) Width of distributions for two dense operators with  $M = \mathcal{D}^{1+\beta}$ , showing the predicted sub-ETH scaling. A dashed line for ETH scaling is also shown.

The RMT correspondence is expected not to work in nonergodic (ETH-violating) systems, e.g., many-body-localized (MBL) systems [14,51–54] and integrable systems. Figures 4(a) and 4(b) show the Hermitian behemoth distribution for an interacting disordered system. At small disorder (ergodic phase), the RMT-predicted exponential is an excellent fit. In the MBL phase, Fig. 4(b), the distribution is a clear power law. This result immediately follows from the power law distribution of eigenstate coefficients known for the MBL phase [53].

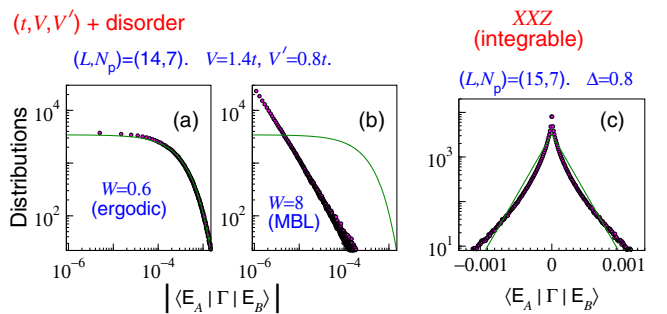


FIG. 4. Distributions for hermitian counterparts of behemoths. (a),(b) A spinless-fermion chain with NN and NNN interactions  $V$  and  $V'$ , subject to Gaussian disorder of strength  $W$ . (a) In the ergodic phase, distribution is exponential as predicted by RMT, Eq. (5). (b) In the many-body localized phase, the distribution is a power law. (c) Integrable XXZ spin chain, showing deviation from RMT prediction.

In integrable systems, local operators have non-ETH scaling (power law with system size) [17,18,55–58]. The behemoths, however, have the same  $\mathcal{D}^{-1}$  scaling as in nonintegrable cases, by normalization. Figure 4(c) shows some deviation from the RMT prediction in the integrable XXZ chain. It is conjectured that the coefficient distribution of integrable systems approaches a power law for  $\mathcal{D} \rightarrow \infty$  [43], which implies that the behemoth distribution also approaches power law behavior. The size-dependence of our data is consistent with this conjecture.

*Discussion.*—In this Letter, we have investigated the matrix element distribution of operators acting on typical midspectrum eigenstates of many-body Hamiltonians. The distributions in nonintegrable many-body interacting models largely match random matrix theory predictions. We have (i) constructed extremely nonlocal operators—behemoths—that satisfy *super*-ETH scaling (width  $\sigma \sim \mathcal{D}^{-1}$  compared to  $\sigma \sim \mathcal{D}^{-1/2}$  for ETH), (ii) interpolated between behemoths and local operators noting that the form of the distribution and its scaling can be captured by RMT but that for local operators there are small departures in the width coming from correlations in the many-body eigenstates, and (iii) obtained a set of typical operators with *sub*-ETH scaling ( $\sigma \sim \mathcal{D}^{-\delta}$  with  $\delta < 1/2$ ).

In closing, we consider the frequency with which different scalings occur in the space of all operators  $\mathbb{O}$  acting on the many-body Hilbert space (Fig. 1). Consider a many-body system with a  $\mathcal{D}$  dimensional Hilbert space and operators  $\hat{\Omega}$  that each contain  $M$  nonzero elements in the configuration basis where  $1 \leq M \leq \mathcal{D}^2$ . The behemoths form a basis in  $\mathbb{O}$  but to facilitate the counting, we consider sums of behemoths with coefficients zero and one—the set of operators living in  $\bar{\mathbb{O}} \subset \mathbb{O}$ . We expect, however, the scalings we have found to hold for arbitrary coefficients of order 1 and for any basis “sufficiently different” from the eigenstate basis. There are then  $2^{\mathcal{D}^2}$  distinct operators in  $\bar{\mathbb{O}}$ . Of these, there are  $\mathcal{D}^2$  Behemoth operators and  $(\log \mathcal{D})^2$  physical two-point local operators. Assuming that the random matrix scaling is obeyed by all typical operators within each class, it follows that super-ETH scaling is observed for  $\sum_{k=1}^{\mathcal{D}-1} \binom{\mathcal{D}^2}{k}$  operators, ETH scaling for  $\binom{\mathcal{D}^2}{\mathcal{D}}$  and sub-ETH scaling for the rest. For large  $\mathcal{D}$  this gives  $\exp[\mathcal{D}(\log \mathcal{D} + 1)]/\sqrt{\mathcal{D}}$  super-ETH operators. The sub-ETH operators appear exponentially more frequently than the rest, while physical operators are doubly exponentially suppressed again in the space of operators with  $\mathcal{D}^{-\delta}$  scaling with  $\delta \geq 1/2$ . From this point of view, typical operators exhibit sub-ETH scaling while ETH scaling is exponentially rare. Both the dominance of sub-ETH operators and the relative rarity of behemoths are compounded when arbitrary coefficients (not only 0 and 1) are allowed [59].

We thank A. Bäcker, Y. Bar Lev, W. Beugeling, M. Kollar, D. Luitz, R. Moessner, H. Nugent, and A. Sen for

helpful discussions. I. M. K. acknowledges the support of German Research Foundation (DFG) Grant No. KH~425/1-1 and the Russian Foundation for Basic Research Grant No. 17-52-12044.

- 
- [1] M. V. Berry, Regular and irregular semiclassical wavefunctions, *J. Phys. A* **10**, 2083 (1977).
  - [2] P. Pechukas, Distribution of Energy Eigenvalues in the Irregular Spectrum, *Phys. Rev. Lett.* **51**, 943 (1983).
  - [3] P. Pechukas, Remarks on “quantum chaos”, *J. Phys. Chem.* **88**, 4823 (1984).
  - [4] A. Peres, Ergodicity and mixing in quantum theory. i, *Phys. Rev. A* **30**, 504 (1984).
  - [5] M. Feingold, N. Moiseyev, and A. Peres, Ergodicity and mixing in quantum theory. ii, *Phys. Rev. A* **30**, 509 (1984).
  - [6] M. Feingold and A. Peres, Distribution of matrix elements of chaotic systems, *Phys. Rev. A* **34**, 591 (1986).
  - [7] R. V. Jensen and R. Shankar, Statistical Behavior in Deterministic Quantum Systems with Few Degrees of Freedom, *Phys. Rev. Lett.* **54**, 1879 (1985).
  - [8] M. Srednicki, Chaos and quantum thermalization, *Phys. Rev. E* **50**, 888 (1994).
  - [9] J. M. Deutsch, Quantum statistical mechanics in a closed system, *Phys. Rev. A* **43**, 2046 (1991).
  - [10] P. Reimann, Eigenstate thermalization: Deutsch's approach and beyond, *New J. Phys.* **17**, 055025 (2015).
  - [11] J. Deutsch, Eigenstate thermalization hypothesis, *Rep. Prog. Phys.* **81**, 082001 (2018).
  - [12] P. Reimann, Dynamical Typicality Approach to Eigenstate Thermalization, *Phys. Rev. Lett.* **120**, 230601 (2018).
  - [13] L. D'Alessio, Y. Kafri, A. Polkovnikov, and M. Rigol, From quantum chaos and eigenstate thermalization to statistical mechanics and thermodynamics, *Adv. Phys.* **65**, 239 (2016).
  - [14] R. Nandkishore and D. A. Huse, Many-body localization and thermalization in quantum statistical mechanics, *Annu. Rev. Condens. Matter Phys.* **6**, 15 (2015).
  - [15] D. A. Abanin, E. Altman, I. Bloch, and M. Serbyn, Ergodicity, Entanglement and Many-Body Localization, [arXiv:1804.11065](https://arxiv.org/abs/1804.11065).
  - [16] C. Neuenhahn and F. Marquardt, Thermalization of interacting fermions and delocalization in fock space, *Phys. Rev. E* **85**, 060101 (2012).
  - [17] W. Beugeling, R. Moessner, and M. Haque, Finite-size scaling of eigenstate thermalization, *Phys. Rev. E* **89**, 042112 (2014).
  - [18] W. Beugeling, R. Moessner, and M. Haque, Off-diagonal matrix elements of local operators in many-body quantum systems, *Phys. Rev. E* **91**, 012144 (2015).
  - [19] M. Rigol, V. Dunjko, and M. Olshanii, Thermalization and its mechanism for generic isolated quantum systems., *Nature (London)* **452**, 854 (2008).
  - [20] M. Rigol, Breakdown of Thermalization in Finite One-Dimensional Systems, *Phys. Rev. Lett.* **103**, 100403 (2009).
  - [21] G. Biroli, C. Kollath, and A. M. Läuchli, Effect of Rare Fluctuations on the Thermalization of Isolated Quantum Systems, *Phys. Rev. Lett.* **105**, 250401 (2010).
  - [22] M. Rigol and L. F. Santos, Quantum chaos and thermalization in gapped systems, *Phys. Rev. A* **82**, 011604 (2010).

- [23] L. F. Santos and M. Rigol, Localization and the effects of symmetries in the thermalization properties of one-dimensional quantum systems, *Phys. Rev. E* **82**, 031130 (2010).
- [24] G. Roux, Finite-size effects in global quantum quenches: Examples from free bosons in an harmonic trap and the one-dimensional Bose-Hubbard model, *Phys. Rev. A* **81**, 053604 (2010).
- [25] A. Motohashi, Thermalization of atom-molecule Bose gases in a double-well potential, *Phys. Rev. A* **84**, 063631 (2011).
- [26] G. P. Brandino, A. De Luca, R. M. Konik, and G. Mussardo, Quench dynamics in randomly generated extended quantum models, *Phys. Rev. B* **85**, 214435 (2012).
- [27] T. N. Ikeda, Y. Watanabe, and M. Ueda, Finite-size scaling analysis of the eigenstate thermalization hypothesis in a one-dimensional interacting Bose gas, *Phys. Rev. E* **87**, 012125 (2013).
- [28] R. Steinigeweg, J. Herbrych, and P. Prelovšek, Eigenstate thermalization within isolated spin-chain systems, *Phys. Rev. E* **87**, 012118 (2013).
- [29] H. Kim, T. N. Ikeda, and D. A. Huse, Testing whether all eigenstates obey the eigenstate thermalization hypothesis, *Phys. Rev. E* **90**, 052105 (2014).
- [30] S. Sorg, L. Vidmar, L. Pollet, and F. Heidrich-Meisner, Relaxation and thermalization in the one-dimensional Bose-Hubbard model: A case study for the interaction quantum quench from the atomic limit, *Phys. Rev. A* **90**, 033606 (2014).
- [31] R. Steinigeweg, A. Khodja, H. Niemeyer, C. Gogolin, and J. Gemmer, Pushing the Limits of the Eigenstate Thermalization Hypothesis Towards Mesoscopic Quantum Systems, *Phys. Rev. Lett.* **112**, 130403 (2014).
- [32] K. R. Fratus and M. Srednicki, Eigenstate thermalization in systems with spontaneously broken symmetry, *Phys. Rev. E* **92**, 040103 (2015).
- [33] R. Mondaini, K. R. Fratus, M. Srednicki, and M. Rigol, Eigenstate thermalization in the two-dimensional transverse field Ising model, *Phys. Rev. E* **93**, 032104 (2016).
- [34] A. Chandran, M. D. Schulz, and F. J. Burnell, The eigenstate thermalization hypothesis in constrained Hilbert spaces: A case study in non-abelian anyon chains, *Phys. Rev. B* **94**, 235122 (2016).
- [35] D. J. Luitz and Y. Bar Lev, Anomalous Thermalization in Ergodic Systems, *Phys. Rev. Lett.* **117**, 170404 (2016).
- [36] R. Mondaini and M. Rigol, Eigenstate thermalization in the two-dimensional transverse field Ising model. ii. off-diagonal matrix elements of observables, *Phys. Rev. E* **96**, 012157 (2017).
- [37] T. Mori, T. N. Ikeda, E. Kaminishi, and M. Ueda, Thermalization and prethermalization in isolated quantum systems: a theoretical overview, *J. Phys. B* **51**, 112001 (2018).
- [38] T. Yoshizawa, E. Iyoda, and T. Sagawa, Numerical Large Deviation Analysis of the Eigenstate Thermalization Hypothesis, *Phys. Rev. Lett.* **120**, 200604 (2018).
- [39] R. Hamazaki and M. Ueda, Atypicality of Most Few-Body Observables, *Phys. Rev. Lett.* **120**, 080603 (2018).
- [40] J. R. Garrison and T. Grover, Does a Single Eigenstate Encode the Full Hamiltonian?, *Phys. Rev. X* **8**, 021026 (2018).
- [41] G. Goldstein and N. Andrei, Strong eigenstate thermalization hypothesis, [arXiv:1408.3589](https://arxiv.org/abs/1408.3589).
- [42] W. Beugeling, A. Andreev, and M. Haque, Global characteristics of all eigenstates of local many-body Hamiltonians: participation ratio and entanglement entropy, *J. Stat. Mech.* (2015) P02002.
- [43] W. Beugeling, A. Bäcker, R. Moessner, and M. Haque, Statistical properties of eigenstate amplitudes in complex quantum systems, *Phys. Rev. E* **98**, 022204 (2018).
- [44] Please refer to Sec. S.III of Ref. [45] for additional expressions for the behemoth operators in terms of creation and annihilation operators.
- [45] See Supplemental Material at <http://link.aps.org/supplemental/10.1103/PhysRevLett.122.070601> for more data and details of calculations.
- [46] The configurations  $\mathbf{n}_j$  and  $\mathbf{n}'_j$  are the ones coupled by the operator  $\hat{\Omega}_M$  and determined by the sets  $\{r_k\}$  and  $\{s_k\}$ . Note that the further analysis is applicable not only for a certain type of nonlocal operators  $\hat{\Omega}_M = \prod_{k=1}^n \hat{c}_{r_k}^\dagger \hat{c}_{s_k}$ , but for general operators  $\hat{\Omega}_M$  with  $M$  nonzero elements.
- [47] M. L. Mehta, *Random Matrices* (Elsevier, New York, 2004).
- [48] C. W. J. Beenakker, Random-matrix theory of quantum transport, *Rev. Mod. Phys.* **69**, 731 (1997).
- [49] T. Guhr, A. Mueller-Groeling, and H. A. Weidenmueller, Random-matrix theories in quantum physics: common concepts, *Phys. Rep.* **299**, 189 (1998).
- [50] F. Evers and A. D. Mirlin, Anderson transitions, *Rev. Mod. Phys.* **80**, 1355 (2008).
- [51] V. Oganesyan and D. A. Huse, Localization of interacting fermions at high temperature, *Phys. Rev. B* **75**, 155111 (2007).
- [52] F. Alet and N. Laflorencie, Many-body localization: an introduction and selected topics, *C.R. Phys.* **19**, 498 (2018).
- [53] A. D. Luca and A. Scardicchio, Ergodicity breaking in a model showing many-body localization, *Europhys. Lett.* **101**, 37003 (2013).
- [54] D. J. Luitz, Long tail distributions near the many-body localization transition, *Phys. Rev. B* **93**, 134201 (2016).
- [55] S. Ziraldo and G. E. Santoro, Relaxation and thermalization after a quantum quench: Why localization is important, *Phys. Rev. B* **87**, 064201 (2013).
- [56] V. Alba, Eigenstate thermalization hypothesis and integrability in quantum spin chains, *Phys. Rev. B* **91**, 155123 (2015).
- [57] S. Nandy, A. Sen, A. Das, and A. Dhar, Eigenstate Gibbs ensemble in integrable quantum systems, *Phys. Rev. B* **94**, 245131 (2016).
- [58] M. Haque and P. McClarty, Eigenstate thermalization scaling in Majorana clusters: from chaotic to integrable Sachdev-Ye-Kitaev models, [arXiv:1711.02360](https://arxiv.org/abs/1711.02360).
- [59] The operator counting can be repeated by allowing the coefficients to assume a discrete number of values  $k+1$  between  $a$  and  $b$  (say  $a, a+(b-a)/k, a+2(b-a)/k, \dots, b$ ). In this case the number of behemoth operators scales as  $O(kD^2)$  while the total number of operators goes as  $(k+1)^{D^2}$ . So the behemoth operators are exponentially more rare in the space of operators as the number of allowed coefficient increases.